Properties of model E-glass fiber composites with varying matrix monomer ratios

Dental Materials xxx (xxxx) xxx

Contents lists available at ScienceDirect

Dental Materials

journal homepage: www.elsevier.com/locate/dental

Properties of model E-glass fiber composites with varying matrix monomer ratios

Abdulrahman Alshabib [a,*], Nikolaos Silikas [b], David C. Watts [b,**]

[a] Department of Restorative Dentistry, College of Dentistry, King Saud University, Riyadh, Saudi Arabia
[b] Dentistry, School of Medical Sciences, University of Manchester, Manchester, UK

ARTICLE INFO

Keywords:
Resin composites
Ethoxylated bisphenol-A-dimethacrylate
UDMA
Fiber reinforcement
Flexural strength
Fracture toughness
Hygroscopic expansion

ABSTRACT

Objective: To evaluate properties of fiber-reinforced-composites (FRC) containing Bis-EMA/UDMA monomers but identical dispersed phase (60% wt BaSi glass power +10% wt E-glass fibre).
Methods: A control (Group A), monomer mixture comprising 60% Bis-GMA, 30% TEGDMA, and 10% PMMA (typical FRC monomers) was used. The following monomer mass fractions were mixed: 50% bis-GMA plus 50% of different ratios of Bis-EMA+UDMA to produce consistent formulations (Groups B-E) of workable viscosities was also studied. Flexural strength (FS), fracture toughness (K_{IC}), water sorption (SP), solubility (SL) and hygroscopic expansion (HE) were measured. FS and K_{IC} specimens were stored for 1, 7 d, and 30 d in water at 37 °C. SP/SL specimens were water-immersed for 168d, weighed at intervals, then dried for 84 d at 37 °C. To analyze differences in FS, and K_{IC}, a two-way ANOVA and Tukey post-hoc tests ($\alpha = 0.05$) were conducted. For SP/SL, and HE, one-way ANOVA with subsequent Tukey post-hoc tests ($\alpha = 0.05$) were utilized.
Results: FS and K_{IC} for groups A, D, E decreased progressively after 1 d. Groups B and C (highest amounts of Bis-EMA) did not decrease significantly. The modified matrix composites performed significantly better than the control group for SP and HE. The control group outperformed the experimental composites only for SL with up to 250% higher SL for group E (6.9 μg/mm) but still below the maximum permissible threshold of 7.5 μg/mm.
Significance:
Experimental: composites with highest amounts of Bis-EMA showed improved hydrolytic stability and overall enhancement in several clinically-relevant properties. This makes them potential candidates for alternative matrices to a semi-interpenetrating network in fiber-reinforced composites.

1. Introduction

It is more than fifty years since resin composites were first employed for clinical use. In the 1980 s and 1990 s, emphasis was placed on particulate filler systems. These led progressively to microhybrid composites that were more resistant to wear and had superior mechanical properties [1]. Over the next decade, attention turned towards reducing polymerization shrinkage to minimize the issues of interfacial gap formation, post-operative sensitivity and cuspal deflection [2]. More recently, bulk-fill composites have gained popularity as they require less time for placement into the cavity preparation [3].

Many reviews exist on resin composite restorations in vital posterior teeth. One review compared studies conducted between 1995 and 2005 with those conducted between 2006 and 2016 [4]. Over the earlier period, reported survival rates were 89.4% compared with 86.9% for the later period, a marginal difference. The reported rates of secondary caries were also similar: 29.5% in 1995–2005, and 25.7% in 2006–2016. However, the frequency of fractures in composite and teeth was significantly higher in 2006–2016. The possible explanation was that composites were employed in larger restorations in this more recent period. Therefore studies have investigated potential ways to enhance the mechanical properties of particulate filled composite (PFC), through various curing techniques [5,6], selection of resin matrices [7], and improving the filler content [1].

In a recent study, the physical properties of fiber reinforced composites (FRCs) were compared with various commercial *particulate filled* composites (PFCs) [8]. The results showed that the mechanical properties of FRC differed considerably from conventional and bulk-fill PFC,

* Correspondence to: King Saud University, Saudi Arabia.
** Correspondence to: University of Manchester, Manchester, UK.
E-mail addresses: abdalshabib@ksu.edu.sa (A. Alshabib), david.watts@manchester.ac.uk (D.C. Watts).

https://doi.org/10.1016/j.dental.2023.12.002
Received 15 November 2023; Received in revised form 8 December 2023; Accepted 8 December 2023

demonstrating superior fracture toughness. Moreover, in vitro fracture resistance of endodontically-treated teeth restored with various core materials was studied by Garlapati et al. [9]. They concluded that fiber reinforced composites provided the highest fracture resistance. However, several factors affect the efficiency of the fiber reinforcement, including: fiber type, orientation, distribution [10,11], aspect ratio [12,13], volume fraction [14] and the chemical bonding between fiber and resin matrix [15,16].

Fiber orientation within the resin is of critical importance due to the isotropic versus anisotropic reinforcement they provide [10,17]. It is more difficult to control the orientation of discontinuous fibers (unidirectional or multidirectional) than continuous (unidirectional or bidirectional) fibers, especially if the discontinuous fibers are oriented in a multidirectional manner. Methods used for evaluating fiber orientation include two-dimensional (2-D) imaging techniques such as optical and scanning-electron microscopy [10]. A drawback of these 2-D methods is the projection of the discontinuous fibers aligned in one plane. This could be resolved by providing sections of the same sample cut in different planes and analysing each of them [10]. However, this method is unreliable because the techniques used for specimen preparation may alter the internal structure. Non-invasive techniques such as μCT scanning could be used to analyse fiber orientation in a 3D projection.

With regard to the use of FRCs in clinical applications, the principal limitation is the few investigations of their long-term clinical performance. Most studies have concerned laboratory measurements of their material properties. The most significant weakness of FRCs is the interface between the resin matrix and the fiber. Intraoral hydrolysis and degradation can lead to failure of the restoration through weakening of this interface [18]. This may explain why there is a lack of long-term studies.

Resin composites are typically characterized by their use of cross-linked thermoset polymer structures. To enhance their surface adhesive properties, the matrix of these composites has been augmented with the addition of linear PMMA polymer. A combination of linear polymer and crosslinked polymer is utilised in a commercially available E-glass FRC (everX™ GC, Japan) [19]. Despite significant improvements in the mechanical properties for short FRC (everX™) [8], there are some drawbacks to the semi-interpenetrating polymer network (SIPN) (bis-GMA/ TEGDMA –PMMA) system, as aqueous storage has a significant negative effect on its properties [18].

Solvents can have different effects on dental composites. When stored in water for 1 or 2 months, the flexural strength of composites undergoes substantial reduction [20,21]. Similarly, water ageing can reduce fracture toughness by 10–35% [22,23]. However, other literature reports that flexural strength or fracture toughness do not change or may even increase when composites are stored in water [24–26].

These conflicting results may be attributed to differences in the materials and methods used, especially the composition of fillers and resins tested. Tanaka et al., studied conventional composites stored in water and found substantial 30% reductions in compressive and diametral tensile strength, flexural strength and elastic modulus. However, when similar tests were conducted on an experimental composite containing a fluorinated polymer, only the flexural strength reduced, highlighting the key role played by the resin components when investigating solvent resistance [27].

This study aims to formulate fiber-containing composites where a semi-interpenetrating polymer network (Bis-GMA-TEGDMA/PMMA) is substituted by a cross-linked resin matrix (Bis-GMA- UDMA/Bis-EMA) at different ratios. These experimental resin composite systems will be studied to evaluate how de-ionized water storage affects their flexural strength, fracture toughness, water sorption, solubility, and hygroscopic expansion.

The null hypotheses are that there are:

1. No differences exist between the control group and the experimental groups: in flexural strength and fracture toughness after water storage at 1 d, 7 d, 30 d at 37 °C.
2. No differences exist between the control group and the experimental groups: in water sorption, solubility, and hygroscopic expansion after 168 d of aqueous exposure at 37 °C.

2. Materials and methods

Monomers and the reinforcing materials used to formulate the experimental groups are listed in Table 1.

2.1. Silane functionalization of Barium borosilicate surfaces

60 ml of ethanol and 20 g of borosilicate particle fillers contained in a plastic container were placed in a SpeedMixer™ (DAC 150.1 FVZK, High Wycombe, Buckinghamshire, UK) and mixed for 20 min at 1500 rpm. Following initial mixing, a sterile syringe was used to slowly add 3% (0.6 g) of the silane coupling agent (3- trimethoxysilyl propyl methacrylate). This mixture was then put back into the Speedmixer for 10 min at 1500 rpm, before being separated equally into two plastic tubes and put into a 4000-rpm centrifuge (Heraeus, UK) for 20 min at 23 °C. The supernatant (separated ethanol) was removed and the silanated fillers was placed in plastic tubes and dried for 3 h in an EZ-2 Elite personal solvent evaporator (Genevac Ltd, SP Scientific Company, UK) at 60 °C. Once dried, the silanated fillers were stored at room temperature (23 °C ± 1).

2.2. Fabrication of filled resin composites

Five resin monomer matrix groups were formulated (Table 2. A digital microbalance (BM-252, A&D Company, Japan) was used to measure the mass of resin. Each group was mixed with CQ (0.5 wt%) and 1 wt% of DMAEMA in a SpeedMixer™ at 1500 rpm for 3 cycles of 5 min

The filler phase was 60 wt% silanated barium borosilicate glass and 10% wt E-glass fiber. This made the weight percentage ratio of monomer to filler 30:70 for all composites.

Table 1
Monomers and reinforcing materials.

Abbreviation	Name	Lot number	Manufacturer
Organic Component			
Bis-GMA	Bisphenol A-glycidyl dimethacrylate	804–39	Esschem, Europe
UDMA	Urethane dimethacrylate	803–66	Esschem, Europe
Bis-EMA (EO=8)	Ethoxylated bisphenol-A dimethacrylate	849–17	Esschem, Europe
TEGDMA	Triethyleneglycol dimethacrylate	807–32	Esschem, Europe
PMMA	Polymethyl methyl methacrylate	93–097	Esschem, Europe
CQ	Camphorquinone	09003 A	Sigma–Aldrich Inc., St. Louis, USA
DMAEMA	Dimethylaminoethyl methacrylate	BCBR4467V	Sigma–Aldrich Inc., St. Louis, USA
Reinforcing component			
BBAS	Barium borosilicate glass: average particle size 0.7 μm	EEG 101–07-/ 871–12	Esschem, Europe
SiO_2	Silica oxide glass: average particle size of 0.7 μm	1332–37	Donghai Changtong Silica Powder Co. Dongjai,China
GF	Silanated E-glass fibers: diam. 15 μm, length 3 mm.	86–792	Hebei Yuniu Fiberglass Manufacturing Co., Ltd, Guangzong, China
3-MPS	3-Trimethoxysilyl Propyl methacrylate	2530–85–0	Sigma–Aldrich Inc., St. Louis, USA

Table 2
Matrix composition (in wt%) for the control (A) and experimental (B, C, D, E) 60%wt silanated barium borosilicate glass and 10%wt E-glass fiber were added. Making the percentage ratio of monomer to filler 30:70 for all composites.

Group	Bis-GMA	TEGDMA	PMMA	Bis-EMA	UDMA
A	59.5%	29.5%	9.5%	———	———
B	49.5%	———	———	37.0%	12.0%
C	49.5%	———	———	29.5%	19.5%
D	49.5%	———	———	24.5%	24.5%
E	49.5%	———	———	19.5%	29.5%

The final mixture was mixed for 20 min using the SpeedMixer at 1500 rpm (5 min/cycle). The experimental resin composite groups are shown in Table 2.

2.3. Fiber length measurements

The fiber manufacturer provided nominal dimensional data on the fibers: diameter of 15 μm; length 3 mm. Experiments were made to measure the length ranges of representative fibers in a small sample.

0.5 g of E-glass fibers were dispersed in 50 ml of ethanol solution using an ultrasonic vibrator. After the evaporation of ethanol the fibers were vacuum sputter coated with Au/Pd alloy 60/40 with a 10 nm layer thickness (Q150T ES, Quorum technologies, UK) for 2 min. SEM (Quanta 650 FEG, FEI company, USA) was used to image the E-glass fibers, before being processed to establish the final fiber lengths using Image-J software [28]. A total of fifty fibers were included in the calculation.

2.4. Flexural strength and Modulus measurement

Five model fiber reinforced resin composite materials were studied (Groups A-E). For each material, a polytetrafluoroethylene (PTFE) mold was used to produce 18 specimens. The dimensions of each beam were 2 × 2×25 mm. A slab of glass (1 mm thickness) was positioned over the mould to ensure that the material was level with the top surface of the mold. The specimens were photo-polymerised for 20 s at six overlapping sections (total of 120 s), by a LED curing unit with measured average tip irradiance of 1200 mW/cm^2 (Elipar S10, 3 M Espe, Seefeld, Germany). Irradiance was verified using a calibrated radiometer after each use of the light curing unit (MARC™ Resin Calibrator, Blue-light Analytics Inc, Halifax, NS, Canada). Small areas of excess composite tended to exist at the edges of the specimen. They were removed by using 320-grit metallographic papers before being put into bottles of distilled water (n = 6), and placed in an incubator at 37 °C for 24 h, 7 d, 30 d. The specimen dimensions were measured using an electronic digital calliper (Powerfix, OWIM GmbH & Co., KG, Germany) with an accuracy of 0.01 mm. The width and height were measured at the centre of the sample and at two different points. The flexural strengths for the specimens were measured by conducting three-point flexural loading using a Universal Testing Machine (Zwick/Roell-2020, 500 N load cell) at 23 ± 1 °C. Each beam specimen was subjected to a central load in a three-point bending mode, at a crosshead speed of 1.0 mm/s, until each fracture point was reached.

After obtaining the fracture loads, flexural strengths (FS) were calculated through the following formula [29]:

$$\boldsymbol{FS} = \frac{3FL}{2BH^2}$$

where F was the maximum load (in Newtons) at the highest point of load-deflection curve; L was the distance between the supports (mm); B was the width of the specimen (mm) and H, the height (mm).

Equation 1: Flexural strength equation.

The elastic modulus was calculated from the slope of the load deflection curve linear region with the following equation [30,31]:

Equation 2: Elastic modulus equation

$$\boldsymbol{E_f} = \frac{L^3F}{4wh^3d}$$

Where w is the width (mm), h is the height (mm) of the specimen, L (mm) is the distance between the supports and d (mm) is the deflection due to load F (N) applied at the middle of the specimen.

2.5. Fracture toughness

For each material, a polytetrafluoroethylene (PTFE)-lined brass mold was used to produce 18 single edge notched (SEN) specimens. The mold conformed to British Standard 54479:1978 [32]. This included a segment of razor blade incorporated in the mould. The dimensions of the beam were 32 × 6×3 mm. The specimens were photo-polymerised for 20 s at six overlapping sections (total of 120 s), by a LED curing unit (as mentioned above). Small volumes of composite excess tended to exist at the edges of the specimen. They were removed using 320-grit metallographic papers followed by wetting the pre-crack with a drop of glycerol. A sharp razor blade was used to further cut the notch with a sliding back-and-forth motion before being stored in small bottles of distilled water (n = 6), and placed in an incubator at 37 °C for 24 h, 7 d, 30 d. Using a stereomicroscope (EMZ-5; Meiji Techno Co. Ltd. Japan), at X 1.5 magnification, the crack length was measured for each specimen to an accuracy of 0.01 mm. The specimen dimensions were measured using an electronic digital calliper (Powerfix, OWIM GmbH & Co., KG, Germany) with an accuracy of 0.01 mm. The width and height were measured at the centre of the sample and at two different points. The K_{IC}, or fracture toughness, for the specimens were measured by flexural loading with a Universal Testing Machine (Zwick/Roell-2020, 500 kN load cell) at 23 ± 1 °C. Each beam specimen was subjected to a central load in a three-point bending mode, at a crosshead speed of 1.0 mm/s, until each specimen's fracture point has been achieved.

From the load values at fracture, fracture toughness was calculated through the following formula [33]:

$$\boldsymbol{K_{IC}} = \left[\frac{PL}{BW^{1.5}} \right] Y$$

P = Load at fracture (in Newtons) B = thickness of the specimen (m).

L = distance between the supports (m) Y = calibration function for given geometry.

W = width of the specimen (m) a = notch length (m).

Equation 3: Fracture toughness equation.

2.6. Scanning electron microscopy (SEM)

SEM images were taken of specimen fracture surfaces of the experimental composites. Specimens were vacuum sputter-coated with Au/Pd alloy 60/40 with a 10 nm layer thickness (Q150T ES, Quorum technologies, UK) for 2 min. Then the fracture sites were observed using a Quanta 650 FEG (FEI Company, USA).

2.7. Micro-CT (μCT) study of fiber orientation

A Teflon mold was used to prepare one specimen beam (3 ×6×34 mm) from groups B, C, and D (with 60% wt Silica oxide and

10% wt E-glass fiber). Each specimen was cured for 120 s from each side using a LED curing unit light curing (as mentioned above). Several overlapping areas of irradiation were utilised along the length of the specimens. Each specimen was placed into the chamber of a μCT (Skyscan 1272 Bruker micro CT, Kontich, Belgium), and was secured in a custom holder for stability throughout the scanning process.

Table 3 provides the details of the parameters used with the μCT.

After scanning, the coronal and sagittal views of each specimen were saved as 16 bit TIFF files (using N-Recon software). CTAn and CTvol software were used, respectively, to convert the images to a 3D image and then to create 3D models of the specimens. All software from Bruker AG, Germany.

2.8. Sorption and solubility

2.8.1. Specimen preparation

Using brass moulds, five disc-shaped specimens were produced for each material. The moulds (15 ×2 mm), were placed between two sections of clear Mylar strip with glass slides on each side (1 mm thick) and then squeezed together. An LED curing unit with measured average tip irradiance of 1.2 W/cm^2 (Elipar S10, 3 M Espe, Seefeld, Germany) was used to irradiate five sections of each side for 20 s. The irradiance was measured every time the light cure unit was utilized, using a calibrated radiometer (MARC™ Resin Calibrator, Blue-light analytics Inc, Halifax, NS, Canada). The specimens were taken out of their moulds with care, and 1000 grit silicon carbide paper was used to smooth out any rough edges. Following this, the specimens were placed in a desiccator containing silica gel at 37 ± 1 °C. After a period of 24 h a precision-calibrated balance was used to weigh each specimen, accurate to ± 0.01 mg (BM-252, A&D Company, Japan). The cycle was duplicated repeatedly until a constant mass was acquired (m1) – i.e. until the mass loss of the specimens was no more than 0.2 mg over 24 h.

For the thickness measurement, a digital caliper was used (Absolute Digimatic, Mitutoyo Corp, Japan) to obtain two measurements of the height. After taking the dimensions of the specimen, the volume (V) was calculated in mm^3 through the following formula:

$$V = \pi r^2 t$$

Equation 4: Volume calculation formula.

Where π = 3.14, r is the radius of cross section; t is the thickness of specimen.

2.8.2. Sorption

All five specimens were submerged in 10 ml of distilled water within separate glass bottles sealed with polyethylene caps. The bottles were kept at 37 °C for 1, 2, 3, 4, 5, 6, 7, 14, 21, 28, 56, 84, 112,140, and 168 d. After each time period, a tweezer was used to take each specimen from the bottles. They were dried using filter paper before being weighed 1 min after removal from the water. The recorded mass is denoted as m_2 (t). All five specimens were then returned to aqueous storage. This was replenished every week, with the total volume of water maintained at 10 ml.

Table 3
Parameters used with μCT in the study.

Parameters	
Voltage	70 KV*
Current	142 μA**
Rotation	180°
Rotation step	0.100 °
Exposure time	1800 ms***
Filter	Al primary beam filter
Scanning time	4 h 42 m 49 s

*Kilovoltage,**Microampere.***Millisecond

2.8.3. Solubility

After the sorption cycle was complete, specimens were dried using a desiccator and weighed at time points of 1, 2, 3, 4, 5, 6, 7, 14, 21, 28, 56 and 84 d. Once the mass loss of the specimens was no more than 0.2 mg within any 24 h period, the constant final mass was then obtained (m_3).

Weight increase W_i (%) and water sorption W_{so} were calculated by:

$$W_i(\%) = 100\left[\frac{m_2 - m_1}{m_1}\right]$$

Equation 5**:** Weight increase calculation formula.

m_1 was the conditioned mass prior to immersion in water; m_2 was the mass after water immersion for 168 d.

$$W_{So} = \left[\frac{m_2 - m_3}{V}\right]$$

Equation 6**:** Water sorption formula.

m_2 was the mass after immersion in water for 168 d; m_3 was the mass after desorption, and V was the volume of the specimen.

The percentage water absorbed by a composite at the end of the storage period was calculated by

$$W_{So}(\%) = \left[\frac{m_2 - m_3}{m_1}\right] \mathrm{X}100$$

Equation 7: Water sorption % formula.

The following equation was used to calculate the solubility (Sol) values:

$$Sol = \left[\frac{m_1 - m_3}{V}\right]$$

Equation 8: Solubility formula.

2.9. Hygroscopic expansion

Hygroscopic dimensional changes were measured in parallel with the water sorption measurements. A custom-built noncontact laser micrometer was used to measure the dimensional changes of the specimen. After each time period, specimens were dried using filter paper then measured 1 min after removal from the water. Mean diameter (d_2) was recorded at each time interval (t), and then returned to aqueous storage. An average of 600 diametral values was recorded for each specimen at each time point.

The percentage diametral change was calculated:

$$d(\%) = \frac{d_{2(t)} - d_1}{d_1} \mathbf{x}100$$

Equation 9: Diametral change formula.

The following equation was used to calculate volumetric change, assuming isotropic expansion behaviour [34]:

$$V \quad (\%) = \left[(1 + \frac{d(\%)}{100})^3 - 1\right] x100$$

Equation 10: Volumetric change calculation formula.

3. Statistical analysis

3.1. Flexural strength and fracture toughness

Data for all groups were collected and analysed statistically using SPSS 23.0 (IBM SPSS Statistics, SPSS Inc., New York, USA). The calculated data were tested regarding normality of the distribution using the Shapiro-Wilk test. Two-way ANOVA, one-way AVOVA and Tukey post-hoc tests (α = 0.05) was performed to identify differences in K_{IC}, Flexural strength and modulus (dependent variable) between different groups and time (independent variables). One-way analysis of variance was conducted at each time at a significance level of ($p \leq 0.05$). The Tukey *Post-hoc* test was used to determine significant differences in

flexural strength, fracture toughness, and modulus between the different groups. All data were subjected to Levene's test of homogeneity of variance following the assumption of equal variances.

3.2. Sorption, solubility, and hygroscopic expansion

Using SPSS 23.0 (IBM SPSS Statistics, SPSS Inc., New York, USA). The mean and standard deviations were calculated for the water solubility, water sorption, hygroscopic expansion and mass change. One-way ANOVA was carried out at 168 d followed by Tukey *post-hoc* tests (at $\alpha = 0.05$) for the hygroscopic expansion, water sorption, and mass change. For the solubility, the same statistical test was applied to evaluate differences in weight after 84 d of desorption cycle.

4. Results

4.1. Fiber length measurement

E-glass fibers length measurements ranged between 0.4 and 3.5 mm with an average length of 2.5 mm. 58% was between 2.00 and 3.5 mm (2.9 mm was the average length). 36% of the fibers were between 1.1 and 1.9 mm (1.8 mm was the average). The remaining 6% were between 0.3 and 1 mm with average length in this group was 0.6 mm. Results are presented in Table 4.

4.2. Flexural strength and modulus

Flexural strength (FS) and Flexural moduli (FM) for the composites evaluated in this study are presented in Table 5 and.

Table 6, and shown graphically in Fig. 1. Two-way ANOVA presented significant interactions ($p < 0.001$) between different groups and time for both flexural modulus and strength. The highest FS both prior to and after storage was seen in group B, followed by group C, while the control group (A) had the lowest values after 30 d of water storage. However, no statistically significant difference in FS was apparent between groups.

FS was significantly influenced by the ageing period (decrease in FS), where baseline readings (1 d) were significant higher than values measured over subsequent time periods ($p \leq 0.05$) except for group B and C which showed no statistically significant difference. FS reduction ranged between 16% for group B, to 29% for group A after 30 d.

4.3. Fracture toughness

Fracture toughness (K_{IC}) for the resin composites are presented in Table 7 and shown graphically in Fig. 2. After 1 day water storage, K_{IC} ranged from 2.8 to 3.4 M.Pa $m^{0.5}$ reducing to between 3.0 and 2.3 M.Pa $m^{0.5}$ after 30 d water storage. Group B showed the highest initial K_{IC} 2.96 M.Pa $m^{0.5}$, while group A showed the lowest: 2.3 M.Pa $m^{0.5}$ (after 30 d). K_{IC} reduced over the ageing period. However, no statistically significant difference in K_{IC} was apparent after 30 d storage except for group A, where the reduction was 25.8%.

Table 4
Measured fiber lengths and aspect ratio. Fiber diameter 15 μm was obtained from the manufacturer.

	Fiber length ranges		
	0.3–1 mm	1–2 mm	2–3.5 mm
Fiber lengths grouped by percentage values (%).	6%	36%	58%
Fiber lengths grouped by average length (mm).	0.6	1.8	2.9
Aspect ratio l/d (Average)	40	120	193

Table 5
Flexural strength mean and (standard deviation) (MPa).

Group	1 D	7 D	30 D	Change %
A	168.3 (13.4)$^{a, 1}$	154.8 (17.6)$^{a, 1}$	120.2 (22.1)$^{a, 2}$	28.7%
B	190.5 (22.3)$^{a, 1}$	185.8 (27.4)$^{a, b, 1}$	160.2 (18.1)$^{a, 1}$	15.9%
C	179.8 (23.3)$^{a, 1}$	182.2 (26.0)$^{a, b, 1}$	149.1 (16.9)$^{a, 1}$	17.0%
D	179.4 (17.3)$^{a, 1}$	145.8 (14.8)$^{a, c, 1}$	136.7 (9.4)$^{a, 2}$	23.8%
E	180.2 (17.0)$^{a, 1}$	146.3 (20.8)$^{a, c, 1}$	134.1 (32.5)$^{a, 2}$	25.6%

At each time interval the same superscript letters indicate no significant difference ($p > 0.05$). For each group same number superscript indicates no significant difference ($p > 0.05$).

Table 6
Flexural modulus mean and (standard deviation) (GPa).

Group	1 D	7 D	30 D
A	14.3 (2.6)^{a}	14.0 (1.4)^{a}	13.3 (1.7)^{a}
B	14.7 (2.2)^{a}	12.8 (1.3)$^{a, c}$	12.9 (1.1)^{a}
C	13.0 (1.9)^{a}	12.1 (1.1)$^{a, c}$	12.3 (1.1)^{a}
D	12.7 (1.6)^{a}	10.6 (2.0)$^{b, c}$	11.2 (2.1)^{a}
E	12.5 (1.0)^{a}	10.6 (1.3)$^{b, c}$	11.1 (1.4)^{a}

At each time interval the same superscript letters indicate no significant difference ($p > 0.05$).

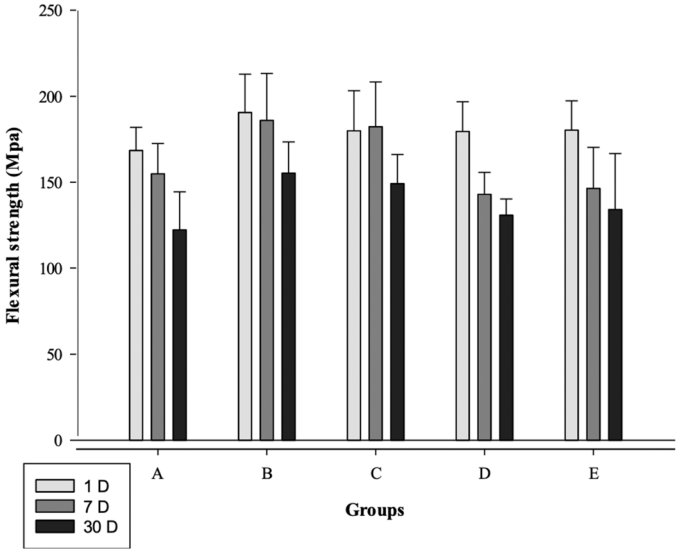

Fig. 1. Flexural strength of composites after 30 d storage in water at 37°C.

Table 7
Fracture toughness K_{IC} mean and (standard deviation) (M.Pa.$m^{0.5}$).

Group	1 D	7 D	30 D	reduction %
A	3.1 (0.45)^{a,1}	2.7 (0.42)^{a,1}	2.3 (0.38)^{a,2}	25.8%
B	3.4 (0.49)^{a,1}	3.0 (0.45)^{a,1}	3.0 (0.48)^{a,1}	11.7%
C	3.0 (0.68)^{a,1}	2.8 (0.31)^{a,1}	2.6 (0.59)^{a,1}	13.3%
D	2.9 (0.38)^{a,1}	2.7 (0.15)^{a,1}	2.5 (0.27)^{a,1}	13.8%
E	2.8 (0.46)^{a,1}	2.5 (0.22)^{a,1}	2.4 (0.45)^{a,1}	14.2%

At each time interval the same superscript letters indicates no significant difference ($p > 0.05$). For each group same number superscript indicates no significant difference ($p > 0.05$).

4.4. SEM of fracture specimens

Representative SEM micrographs of fractured specimens (FS) are shown in Figs. 3 and 4. These show fiber bridging, fiber pull out and fiber breakage at the point of fracture.

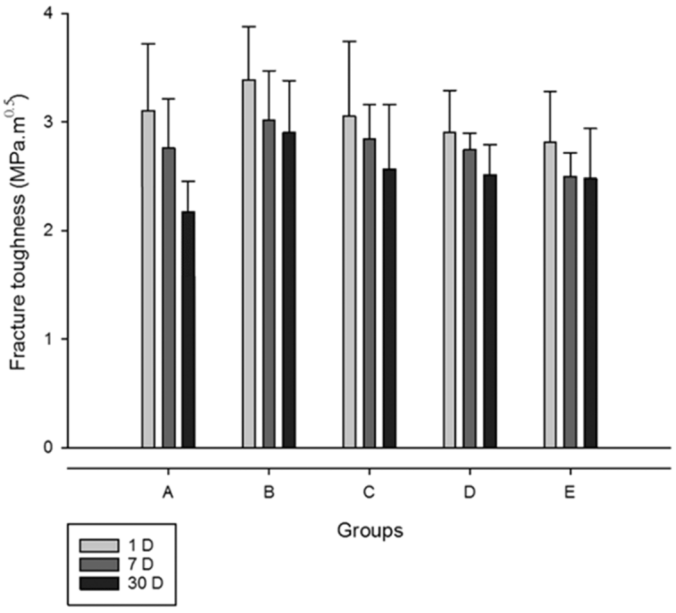

Fig. 2. Fracture toughness of the experimental resin composites after 30 d storage in water at 37°C.

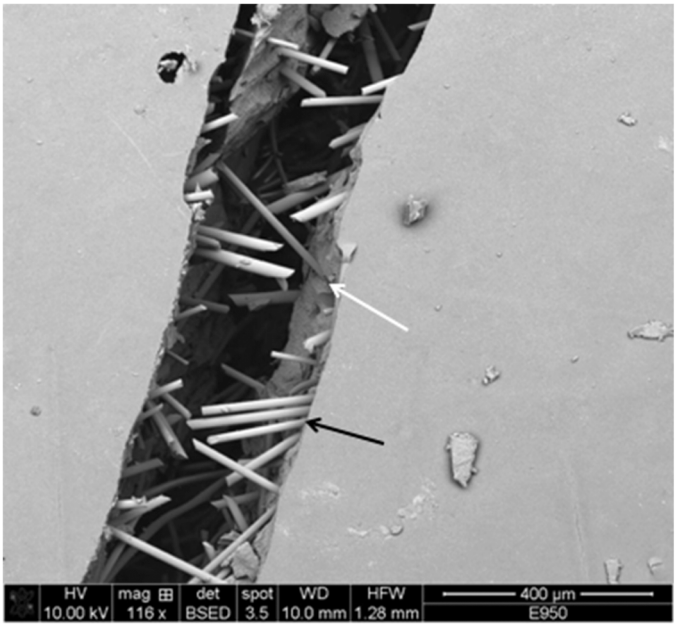

Fig. 3. *:* Fracture surface of the experimental fiber reinforced composite (group B), obtained in back scattered electron mode at × 116 magnification, showing fiber pull-out (black arrow) and fiber bridging (white arrow).

4.5. Fiber orientation

The µCT images (Fig. 5) showed that the short fibers were randomly aligned:

a. viewed parallel to the long axis of the specimen (black arrows);.

b. viewed transverse (perpendicular) to the long axis of the specimen (red arrows).

4.6. Sorption and solubility

As can be seen from Fig. 6, each of the resin composites exhibited a percentage mass change throughout the water sorption/desorption cycle. All of the composites demonstrated increases in mass to varying extents by their water uptake up to the point of equilibrium which occurred after 168 d.

At 168 d, water sorption ranged between 22.62 and 37.89 µg/mm (Table 8). The highest sorption was observed in group A. By contrast, groups, B, C, D and E exhibited lower water sorptions, with no significant differences between these groups ($p \geq 0.05$). Fig. 7.

The solubility for the composites ranged between 2.77 and 6.90 µg/mm, as shown in Table 8. Groups D and E had significantly higher levels of solubility.Fig. 8.

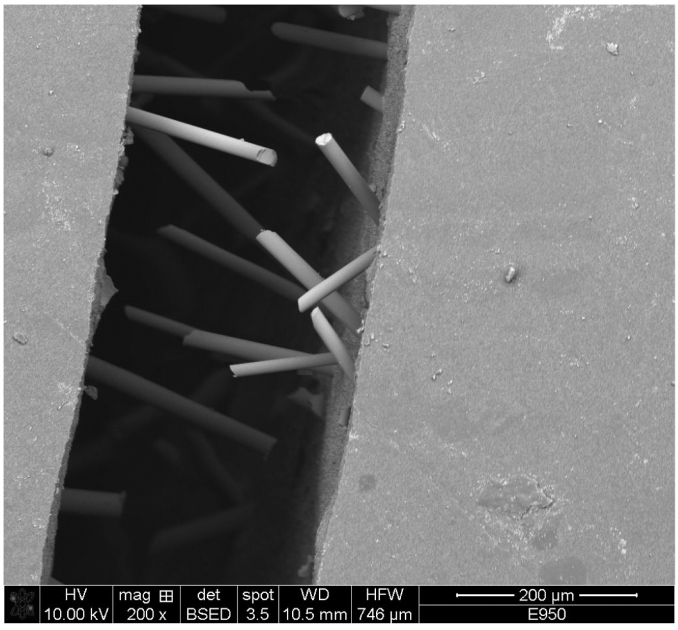

Fig. 4. Fracture surface of the experimental fiber reinforced composite (group B), obtained in back scattered electron mode, x 200, showing random orientation of fibers.

4.7. Hygroscopic expansion

One-way ANOVA conducted after 168 d of immersion in water showed that group A had a significantly higher hygroscopic expansion when compared to the rest of the materials.

The percentage hygroscopic expansion for each material is shown in Fig. 9. The final hygroscopic expansions ranged between 1.23% and 1.71% at 168 d. The highest volumetric change was observed in group A. while groups, B, C, and D exhibited lower volumetric change, with no significant differences between each other ($p \geq 0.05$).

5. Discussion

This study measured the fiber length, flexural strength (FS) and fracture toughness (K_{IC}), water sorption (SP), solubility (SL) and hygroscopic expansion (HE) of experimental fiber-reinforced composites. Both mechanical and water uptake properties were significantly influenced by water storage, leading to the rejection of both null hypotheses.

5.1. Flexural strength and fracture toughness

Recent reports about the clinical performance of resin composite have shown satisfactory survival rates in restorations that are small or medium in size [35,36]. Their annual failure rates are between 1% and 3% [35,37]. The most common causes of failure are recurrent caries and fractures [35,38]. There is a strong correlation between the size of the restoration and the likelihood of it failing [39]. Annual failure rates for

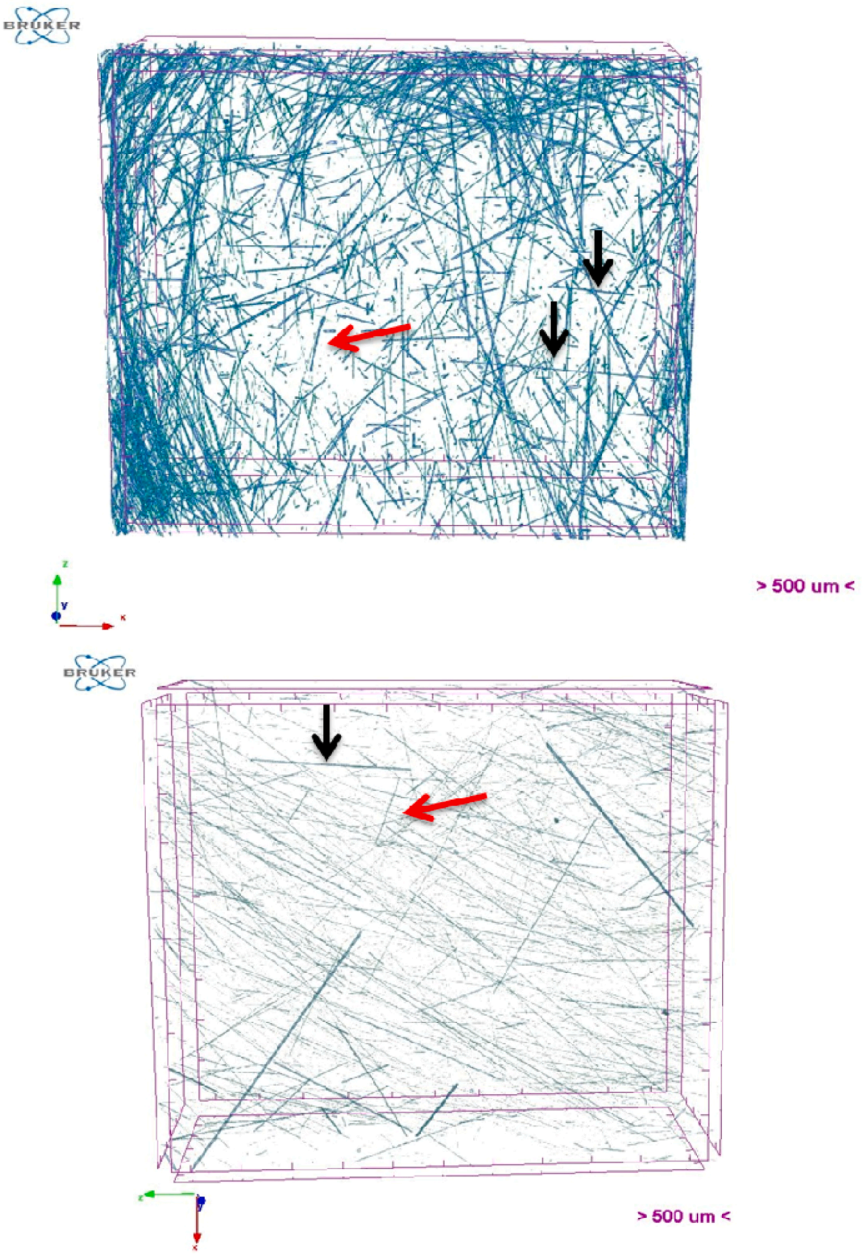

Fig. 5. μCT images of specimens of groups B and C. Black arrows indicate parallel and red arrows indicate perpendicular fiber orientations to the long axis.

single surface restorations are lower (0.94%) than those for four or more surface restorations (9.43%) [39]. The longevity of large restorations is lower because they are more susceptible to failures relating to fractures [40]. This susceptibility to fracture may be associated with the strength of the composite material and patient-related factors such as bruxism [35].

To improve the mechanical properties and load bearing capacity of resin composite, attempts have been made to reinforce the resin phase with glass fibers [41–43]. Fiber reinforcement improves the stress distribution more effectively when loads are concentrated on the restoration [44]. Also, when combining both particles and fibers for reinforcement, improvements were found in both physical (shrinkage stress) and mechanical properties (fracture toughness) in comparison to particulate-only composites [8,44,45].

Previous studies have shown that discontinuous fibers have generally lower strength than with continuous fibers [46,47]. However, when the length of the discontinuous fibers exceeds a critical value, discontinuous fibers can promote a comparable strength [12]. The aspect ratio of fibers is closely linked to the critical fiber length. This may be defined as the minimum fiber length required for optimal stress transfer within the resin matrix [48]. This length is equivalent to the minimum length at which a fiber will fail, midway along its length in an FRC, rather than by interfacial fracture between the matrix and the fiber [47]. In FRC, the critical fiber length should be 50 times greater than the diameter of the fiber, to allow homogenous stress transfer within the resin matrix [47]. The diameter of E-glass fibers used in this study was 15 μm, therefore the critical length should be over 0.75 mm. In this study the majority (94%) of the fibers were above the critical fiber length, and most of them (58%) were between 2 mm and 3.5 mm.

The experimental FRC possessed high resistance to the propagation of cracks. Fig. 3 illustrates the phenomenon of crack bridging (white arrow), where discontinuous fibers stretch over the edges of the crack. This reduces the strain in the notch and blunts the sharp crack. There is therefore less stress at the tip of the crack, so crack propagation is slowed

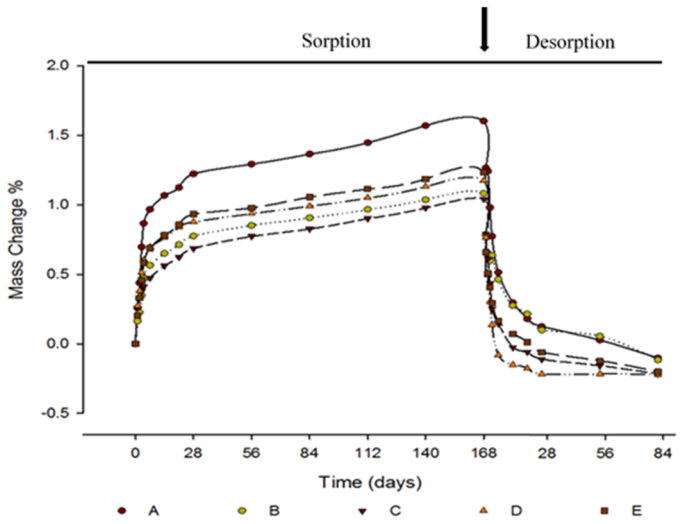

Fig. 6. Mass changes with water sorption and desorption cycles.

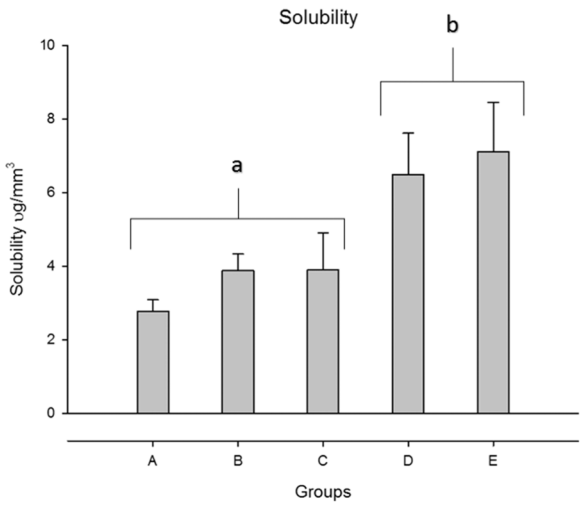

Fig. 8. Solubility of the resin composites after storage in distilled water for 168 days. The same lowercase letters indicate a homogeneous subset ($p > 0.05$).

Table 8
Water sorption (WS) and solubility (SL), and percentage increase in mass and volume, of the experimental FRC after 168 d storage in distilled water at 37°C.

Materials	% Mass increase	Wso (μg/mm^3)	Sol (μg/mm^3)	% Volumetric increase
A	1.60 (0.30)^a	37.89 (2.88)^a	2.77 (0.31)^a	1.71 (0.21)^a
B	0.90 (0.09)^b	22.62 (2.76)^b	3.87 (0.46)^a	1.23 (0.23)^b
C	0.86 (0.15)^b	22.70 (3.02)^b	3.90 (1.00)^a	1.34 (0.16)^b
D	0.94 (0.17)^b	25.64 (3.44)^b	6.48 (1.13)^b	1.32 (0.06)^b
E	1.03 (0.15)^b	29.60 (2.83)^b	6.90 (1.35)^b	1.42 (0.08)$^{a,\ b}$

The same superscript lowercase letters indicate a homogeneous subset (columns) ($p > 0.05$)

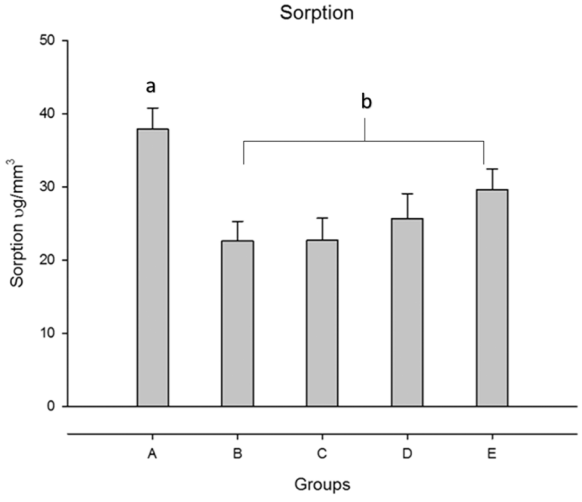

Fig. 7. Sorption of composites after storage in distilled water for 168 days. The same lowercase letters indicate a homogeneous subset ($p > 0.05$).

down or stopped.

Previous research has shown that the FS of resin composites was reduced when stored in water [22,49]. But, other studies did not find a significant change in FS and K_{IC} after water storage [8,50]. These conflicting results may be due to differences in filler particle sizes, the degree of conversion or the interfaces between the filler and matrix.

In this study, storage for 30 d in water decreased FS and K_{IC} of the experimental FRC. To understand the mechanism of degradation in resin

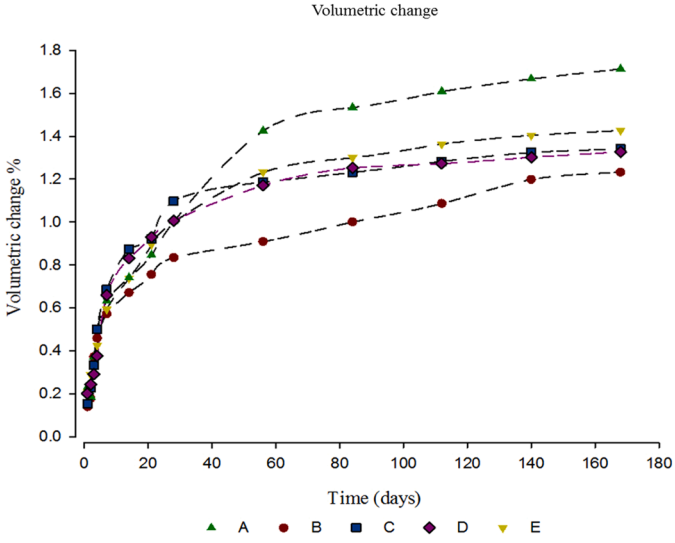

Fig. 9. Hygroscopic expansion from 1 d to 168 d.

composites, synergistic pathways should be considered. For example, the cracks associated with stress crazing open up fresh surface area to reaction. Swelling and water uptake can similarly increase the number of sites for reaction. Degradation products can alter the local pH, stimulating further reaction [44]. For Group A (control group), the effect of water on this composite after 30 d was 29% reduction in FS and 26% in K_{IC}. An explanation is that the control FRC could have higher water sorption, which is related to the hydrophilicity of the polymer network (TEGDMA and PMMA) [51–53]. Moreover, group A had a semi-interpenetrated network (SIPN) matrix, within which thermoplastic PMMA chains are more prone to crazing and crack formation compared to thermoset polymers [54,55].

Groups B and C showed better degradation resistance properties than the other groups of materials. Group B showed the least reduction with water-exposure among all the investigated groups (FS 12% reduction and K_{IC} 14% reduction) after 30 d of water storage. This could be due to a relatively more hydrophobic resin matrix, and higher degree of conversion especially when compared to groups (D and E). This finding is in agreement with a previous study that reported improvement in degradation resistance of Bis-GMA/Bis-EMA mixtures [7].

The placement of composite in a cavity may result in changing the

fiber orientation [11]. For instance, the filling technique and matrix viscosity can modify the fiber arrangement from the random orientation to a more planar orientation that causes anisotropic reinforcement [56]. The length of the fibers and size of the cavity influence the discontinuous-FRC[11]. When cavities have smaller width compared to fiber-length during composite placement, the fibers are arranged in the cavity plane (planar-directional); hence leading to anisotropic features. Multidirectional arrangements of the fiber leading to isotropic properties are enhanced by shorter-scale fibers [10]. To render the three-dimensional images to observe the fiber orientations, radiopaque BBAS fillers were replaced with SiO_2 which is less radiopaque when compared to BBAS, allowing for a distinction in X-ray opacity for the fibers. Specimens were fabricated with 3 mm height and 6 mm width to resemble a clinical scenario of a core build up. Random orientation of the fibers was observed suggesting that isotropic reinforcement could result in such a scenario.

5.2. Sorption, solubility and Hygroscopic expansion

Sorption, through swelling, can have a positive effect, by reducing the material's polymerization stress through expansion. But it also produces negative effects as it may increase monomer leaching and accelerate material degradation [57,58].

Under ISO Standard 4049, it is permissible for a material to possess a sorption limit of 40 μg/mm and solubility of less than 7.5 μg/mm, after it has been stored for 7 days. All of the investigated composites complied with this requirement, although the storage period was much longer, and thus the aqueous challenge more rigorous, than ISO 4049.

The results have shown that the experimental FRC have varying levels of sorption, solubility and volumetric change, depending on the type and amount of monomer used, therefore we rejected the null hypotheses. The sorption of Group A was the highest at 37.8 $\mu g/mm^3$ and that of group B (containing the highest amount of Bis-EMA) was the lowest at 22.6 $\mu g/mm^3$. This suggests that water storage has a significant effect on these polymeric matrices, which is in line with prior work on dimethacrylate-based composites [59,60].

Secondary forces such as intermolecular bonds determine a number of physical properties of a material, for example its sorption, solubility and glass transition temperature [61]. Hydrogen bonds are – cumulatively - the strongest intermolecular force, because of the great number of such bonds that may be present in some polymer/solvent systems. Bis-GMA monomer forms strong hydrogen bonds with water because the presence of –OH group. Thus, Bis-EMA and UDMA will form weaker bonds with water due to the absence of –OH group [62,63]. Sankarapandian et al. [64] also noted that lower water uptake occurred in ethoxylated monomers lacking the hydroxyl group.

Two commercially available composites, Z100 and Z250, contained copolymer bis-GMA/TEGDMA and bis-GMA/bis-EMA/UDMA, respectively. The water sorption of Z100 was 16.85 $\mu g/mm^3$ and for Z250 was 13.02 $\mu g/mm^3$ [62]. This outcome is comparable to our present study as water sorption was lower for groups (B, C, D and E) than for the control group A. The greatest relative increase in sorption was observed in the control group (with TEGDMA and PMMA), while the lowest was observed in group B (with the highest bis-EMA content). Therefore, as the content of bis-EMA decreased, the sorption increased. Composites based on bis-EMA and UDMA monomers should thus present reduced sorption than those with TEGDMA and PMMA.

The second null hypothesis was rejected because the final hygroscopic expansions showed significant variation. Group A had the highest increase (1.71%), whilst other groups had reduced expansions. Hygroscopic expansion occurs when water enters the polymer network, attracted by hydrophilic groups [65,66]. Water diffuses through the organic matrix which expands to accommodate it [67]. Several factors influence this process: monomer structure and chemistry, the fillers employed, porosity of the network and its degree of cross-linking [68]. A material's elastic modulus is important indicator of the extent of expansion; a low modulus is required to allow the polymer phase to accommodate the expansion. The ratio of the hydrophilic attraction to elastic modulus may therefore govern to what extent the dimensions of the polymer phase can be altered. It may be clinically desirable to employ a material that expands with water sorption if this expansion counterbalances the effects of shrinkage. However, it is not desirable to have an expansion coefficient that exceeds the shrinkage value as this can lead to further stresses witthin the teeth.

6. Conclusion

Since the volume fraction and types of filler were identical in all groups, the experimental matrix compositions and monomer ratios significantly influenced the mechanical properties and evidently increased the water degradation resistance of the composites. Groups B and C had favourable outcomes in flexural strength, fracture toughness and degradation resistance. Their improved hydrolytic stability and enhancement in flexural strength may make them potential candidates for alternative matrices in fiber-reinforced composites.

Declaration of Competing Interest

The authors declare no conflict of interest.

Acknowledgement

The authors extend their appreciation to the deputyship for research and innovation of the Ministry of Education in Saudi Arabia for funding this research under grant number IFKSUOR3-168-3.

References

[1] Ferracane JL. Resin composite—state of the art. Dent Mater 2011;27:29–38.
[2] Braga RR, Ferracane JL. Alternatives in polymerization contraction stress management. Crit Rev Oral Biol M 2004;15:176–84.
[3] Chesterman J, Jowett A, Gallacher A, Nixon P. Bulk-fill resin-based composite restorative materials: a review. Br Dent J 2017;222:337–44.
[4] Alvanforoush N, Palamara J, Wong R, Burrow M. Comparison between published clinical success of direct resin composite restorations in vital posterior teeth in 1995–2005 and 2006–2016 periods. Aust Dent J 2017;62:132–45.
[5] Lovell LG, Lu H, Elliott JE, Stansbury JW, Bowman CN. The effect of cure rate on the mechanical properties of dental resins. Dent Mater 2001;17:504–11.
[6] Hughes KO, Powell KJ, Hill AE, Tantbirojn D, Versluis A. Delayed photoactivation of dual-cure composites: effect on cuspal flexure, depth-of-cure, and mechanical properties. Oper Dent 2019;44:E97–104.
[7] Pfeifer CS, Silva LR, Kawano Y, Braga RR. Bis-GMA co-polymerizations: influence on conversion, flexural properties, fracture toughness and susceptibility to ethanol degradation of experimental composites. Dent Mater 2009;25:1136–41.
[8] Alshabib A, Silikas N, Watts DC. Hardness and fracture toughness of resin-composite materials with and without fibers. Dent Mater 2019;35:1194–203.
[9] Garlapati T, Krithikadatta J, Natanasabapathy V. Fracture resistance of endodontically treated teeth restored with short fiber composite used as a core material—An in vitro study. J Prosthodont Res 2017;61:464–70.
[10] Bijelic-Donova J, Garoushi S, Lassila LV, Keulemans F, Vallittu PK. Mechanical and structural characterization of discontinuous fiber-reinforced dental resin composite. J Dent 2016;52:70–8.
[11] Alshabib A, Jurado CA, Tsujimoto A. Short fiber-reinforced resin-based composites (SFRCs); Current status and future perspectives. Dent Mater J 2022;41:647–54.
[12] Shouha P, Swain M, Ellakwa A. The effect of fiber aspect ratio and volume loading on the flexural properties of flowable dental composite. Dent Mater 2014;30:1234–44.
[13] Alshabib A, Silikas N, Algamaiah H, Alayad AS, Alawaji R, Almogbel S, et al. Effect of fibres on physico-mechanical properties of bulk-fill resin composites. Polymers 2023;15:3452.
[14] Berger H, Kari S, Gabbert U, Ramos RR, Castillero JB, Diaz RG. Evaluation of effective material properties of randomly distributed short cylindrical fiber composites using a numerical homogenization technique. J Mech Mater Struct 2007;2:1561–70.
[15] Bae JM, Kim KN, Hattori M, Hasegawa K, Yoshinari M, Kawada E, et al. The flexural properties of fiber-reinforced composite with light-polymerized polymer matrix. Int J Prosthodont 2001;14:33–9.
[16] Matinlinna JP, Lung CYK, Tsoi JKH. Silane adhesion mechanism in dental applications and surface treatments: a review. Dent Mater 2018;34:13–28.
[17] Moezizadeh M, Shokripour M. Effect of fiber orientation and type of restorative material on fracture strength of the tooth. J Conserv Dent: JCD 2011;14:341.

[18] Scribante A, Vallittu PK, Ozcan M, Lassila LVJ, Gandini P, Sfondrini MF. Travel beyond clinical uses of fiber reinforced composites (FRCs) in Dentistry: a review of past employments, present applications, and future perspectives. Biomed Res Int 2018;2018:1498901.
[19] Garoushi S, Sailynoja E, Vallittu PK, Lassila L. Physical properties and depth of cure of a new short fiber reinforced composite. Dent Mater 2013;29:835–41.
[20] Øysæd H, Ruyter IE. Composites for use in posterior teeth: mechanical properties tested under dry and wet conditions. J Biomed Mater Res 1986;20:261–71.
[21] Ferracane J, Berge H, Condon J. In vitro aging of dental composites in water—effect of degree of conversion, filler volume, and filler/matrix coupling. J Biomed Mater Res 1998;42:465–72.
[22] Mair LH, Vowles R. The effect of thermal cycling on the fracture toughness of seven composite restorative materials. Dent Mater 1989;5:23–6.
[23] Algamaiah H, Danso R, Banas J, Armstrong SR, Whang K, Rawls HR, et al. The effect of aging methods on the fracture toughness and physical stability of an oxirane/acrylate, ormocer, and Bis-GMA-based resin composites. Clin Oral Investig 2020;24:369–75.
[24] Drummond JL, Savers EE. In vitro aging of a heat/pressure-cured composite. Dent Mater 1993;9:214–6.
[25] Fujishima A, Miyazaki T, Aoyama M, Suzuki E, Miyaji T, Syafiuddin T. Fracture toughness and fracture behavior of composite resins for posterior restorative materials. Jpn J Conserv Dent 1991;34:45–53.
[26] Janda R, Roulet JF, Latta M, Ruttermann S. The effects of thermocycling on the flexural strength and flexural modulus of modern resin-based filling materials. Dent Mater 2006;22:1103–8.
[27] Tanaka J, Inoue K, Masamura H, Matsumura K, Nakai H, Inoue K. The application of fluorinated aromatic dimethacrylates to experimental light-cured radiopaque composite resin, containing barium-borosilicate glass filler–a progress in nonwaterdegradable properties. Dent Mater J 1993;12:1–11.
[28] Schneider CA, Rasband WS, Eliceiri KW. NIH Image to ImageJ: 25 years of image analysis. Nat Methods 2012;9:671–5.
[29] Standard I. 4049, 2009, Dentistry–Polymer-based restorative materials. International Organization for Standardization, Geneva, Switzerland. 2009.
[30] Asmussen E, Peutzfeldt A. Flexural strength and modulus of a step-cured resin composite. Acta Odontol Scand 2004;62:87–90.
[31] Kakuta K, Urapepon S, Miyagawa Y, Ogura H, Yamanaka M, Suchatlampong C, et al. Development of metal-resin composite restorative material. Part 4. Flexural strength and flexural modulus of metal-resin composite using Ag-In alloy particles as filler. Dent Mater J 2002;21:181–90.
[32] Astm E. 399-90:" standard test method for plane-strain fracture toughness of metallic materials. Annu Book ASTM Stand 1997;3:506–36.
[33] Lloyd CH, Iannetta RV. The fracture toughness of dental composites. I. The development of strength and fracture toughness. J Oral Rehabil 1982;9:55–66.
[34] Martin N, Jedynakiewicz N. Measurement of water sorption in dental composites. Biomaterials 1998;19:77–83.
[35] Demarco FF, Corrêa MB, Cenci MS, Moraes RR, Opdam NJ. Longevity of posterior composite restorations: not only a matter of materials. Dent Mater 2012;28:87–101.
[36] Demarco FF, Collares K, Coelho-de-Souza FH, Correa MB, Cenci MS, Moraes RR, et al. Anterior composite restorations: a systematic review on long-term survival and reasons for failure. Dent Mater 2015;31:1214–24.
[37] Manhart J, Chen H, Hamm G, Hickel R. Buonocore memorial lecture. review of the clinical survival of direct and indirect restorations in posterior teeth of the permanent dentition. Oper Dent 2004;29:481–508.
[38] Brunthaler A, König F, Lucas T, Sperr W, Schedle A. Longevity of direct resin composite restorations in posterior teeth: a review. Clin Oral Investig 2003;7:63–70.
[39] Bernardo M, Luis H, Martin MD, Leroux BG, Rue T, Leitao J, et al. Survival and reasons for failure of amalgam versus composite posterior restorations placed in a randomized clinical trial. J Am Dent Assoc 2007;138:775–83.
[40] Opdam NJ, Bronkhorst EM, Roeters JM, Loomans BA. A retrospective clinical study on longevity of posterior composite and amalgam restorations. Dent Mater 2007;23:2–8.
[41] Smith DC. Recent developments and prospects in dental polymers. J Prosthet Dent 1962;12:1066.
[42] Garoushi S, Vallittu PK, Lassila LV. Fracture resistance of short, randomly oriented, glass fiber-reinforced composite premolar crowns. Acta Biomater 2007;3:779–84.
[43] Fonseca RB, Marques AS, Bernades Kde O, Carlo HL, Naves LZ. Effect of glass fiber incorporation on flexural properties of experimental composites. Biomed Res Int 2014;2014:542678.
[44] Drummond JL. Degradation, fatigue, and failure of resin dental composite materials. J Dent Res 2008;87:710–9.
[45] Garoushi S, Vallittu PK, Watts DC, Lassila LV. Polymerization shrinkage of experimental short glass fiber-reinforced composite with semi-inter penetrating polymer network matrix. Dent Mater 2008;24:211–5.
[46] Chen L, Yu Q, Wang Y, Li H. BisGMA/TEGDMA dental composite containing high aspect-ratio hydroxyapatite nanofibers. Dent Mater 2011;27:1187–95.
[47] Vallittu PK. High-aspect ratio fillers: fiber-reinforced composites and their anisotropic properties. Dent Mater 2015;31:1–7.
[48] Lee SM. Handbook of composite reinforcements. John Wiley & Sons; 1992.
[49] Pilliar RM, Smith DC, Maric B. Fracture toughness of dental composites determined using the short-rod fracture toughness test. J Dent Res 1986;65:1308–14.
[50] ÜÇTAŞLI S, Wilson H, Zaimoglu L. Variables affecting the fracture toughness of resin-based inlay/onlay systems. J Oral Rehabil 1993;20:423–31.
[51] Al Sunbul H, Silikas N, Watts DC. Surface and bulk properties of dental resin-composites after solvent storage. Dent Mater 2016;32:987–97.
[52] Vallittu PK, Ruyter IE, Ekstrand K. Effect of water storage on the flexural properties of E-glass and silica fiber acrylic resin composite. Int J Prosthodont 1998;11:340–50.
[53] Abdel-Magid B, Ziaee S, Gass K, Schneider M. The combined effects of load, moisture and temperature on the properties of E-glass/epoxy composites. Compos Struct 2005;71:320–6.
[54] Wollff E. The effect of cross-linking agents on acrylic resins. J Aust Dent J 1962;7:439–44.
[55] McCabe JF, Wilson HJ. Polymers in dentistry. J Oral Rehabil 1974;1:335–51.
[56] Dyer SR, Lassila LV, Jokinen M, Vallittu PK. Effect of fiber position and orientation on fracture load of fiber-reinforced composite. Dent Mater 2004;20:947–55.
[57] Gopferich A. Mechanisms of polymer degradation and erosion. Biomaterials 1996;17:103–14.
[58] Ferracane JL, Hilton TJ, Stansbury JW, Watts DC, Silikas N, Ilie N, et al. Academy of dental materials guidance-resin composites: part ii-technique sensitivity (handling, polymerization, dimensional changes). Dent Mater 2017;33:1171–91.
[59] Alshali RZ, Salim NA, Satterthwaite JD, Silikas N. Long-term sorption and solubility of bulk-fill and conventional resin-composites in water and artificial saliva. J Dent 2015;43:1511–8.
[60] Al Sunbul H, Silikas N, Watts DC. Resin-based composites show similar kinetic profiles for dimensional change and recovery with solvent storage. Dent Mater 2015;31:e201–17.
[61] Sakaguchi RL, Peters MC, Nelson SR, Douglas WH, Poort HW. Effects of polymerization contraction in composite restorations. J Dent 1992;20:178–82.
[62] Sideridou I, Tserki V, Papanastasiou G. Study of water sorption, solubility and modulus of elasticity of light-cured dimethacrylate-based dental resins. Biomaterials 2003;24:655–65.
[63] Peutzfeldt A. Resin composites in dentistry: the monomer systems. Eur J Oral Sci 1997;105:97–116.
[64] Sankarapandian M, Shobha HK, Kalachandra S, McGrath JE, Taylor DF. Characterization of some aromatic dimethacrylates for dental composite applications. J Mater Sci-Mater M 1997;8:465–8.
[65] Alrahlah A, Silikas N, Watts DC. Hygroscopic expansion kinetics of dental resin-composites. Dent Mater 2014;30:143–8.
[66] Sideridou ID, Karabela MM, Vouvoudi E. Volumetric dimensional changes of dental light-cured dimethacrylate resins after sorption of water or ethanol. Dent Mater 2008;24:1131–6.
[67] Braden M, Davy KWM. Water absorption characteristics of some unfilled resins. Biomaterials 1986;7:474–5.
[68] Moszner N, Salz U. New developments of polymeric dental composites. Prog Polym Sci 2001;26:535–76.